Guided waves for inspection and nondestructive evaluation NDE of tubular structures

Elhadji Barra NDIAYE, Philippe GUY, Thomas MONNIER

Laboratoire Vibrations-Acoustique – INSA de Lyon
25 bis Avenue Jean Capelle, F–69621 Villeurbanne Cedex, France
{elhadji-barra.ndiaye, philippe.guy, thomas.monnier}@insa-lyon.fr

Abstract

In many industrial domains, like chemistry, petrochemistry, gaz or water transportation, products are stored for long durations before their delivery. The storage units are submitted to environmental stresses (temperature and humidity variations, corrosion etc.). It is then important to have reliable tools to evaluate their health state and to detect as soon as possible the occurrence of damages.
Guided waves methods are good candidates to fulfil these inspections. The guided waves that can propagate on cylindrical structures are multimodal and dispersive. They are generally classified in three families, denoted torsional, longitudinal and flexural modes, according to their polarization.
In this paper, we will study the ability of ultrasonic guided modes to detect and localize a lack or an excess of coating on metallic tubes. First of we will study the dispersion curves of an aluminum tube and of a coated aluminum one. From this analysis we will show that the T(0,1) torsional mode is slightly dispersive at a frequency of 100kHz) on the considered structures, and can be used for the considered inspection.
Then we will discuss the results of several finite elements method simulations made with Comsol Multiphysics© for the two kind of structures. From the computed data, we will extract B-scans in the time-position plane. The analyses of these B-scans, allow visualizing the different modes that propagate along the tubes. The influence of a circumferential strip of resin will be shown and discussed.
Then after applying a spatial Fast Fourier Transform with sliding window of these B-scans, we get images in the position–wavenumber (z, k) space. It will be shown that this kind of signal processing enables to detect and localize the presence of the resin strip. So the feasibility of an SHM approach based on guided modes is shown for the considered flaw.
Finally, we will show how a practical SHM method can be implemented based on the previous results.

1 Introduction

The use of ultrasonic guided waves for testing and screening for corrosion or other defects in several types of structures (plates, pipelines, railways, etc.) is increasing nowadays [1–3]. In the petrochemical industry for example, pipelines and other tubular structures are used for the supply and distribution of the required materials (oil, gases etc.). They usually achieve a very long operating life of some decades and a wide variety of damage and aging defects may occur. Cylindrical guided waves techniques have a main advantage that they can propagate over very long distances along structures compared to bulk waves which are just able to test a small area in the vicinity of each source (transducer). Traditional ultrasonic testing which require the use of an internal probe running through the pipe, find difficulty to detect localized corrosion, coating and many other defects but using guided waves allows not only for defect screening but also for defect sizing.

Pochhammer and Chree have earlier provided the mathematical treatment (PC frequency equations) of mechanical wave propagation in cylindrical structures but its complexity prevented researchers from obtaining quantitative results until the development of computer science. Gazis [4] proposed the first exact solutions of the PC frequency equations and a complete description of propagation modes and displacement and stress distributions for an isotropic elastic tube were found later. Hence, the use of the semi-analytical finite element (SAFE) methods to find the waveguide behaviour with the different types of modes becomes possible.

The objective of the present paper is to simulate a guided-wave-based approach Structural Health Monitoring (SHM) and Non Destructive Testing/Evaluation (NDT/E) of an aluminum tube with an axisymmetric resin deposit growing over the time due to aging. At this point, it seems worthwhile to introduce the strategies of SHM and NDT/E. According to Rose [5–6], NDT is difficult as you carry equipment to a site and are asked to find defects in often very complex structures and for SHM, on an other hand, a baseline is available that can often handle very complex structures. The T(0,1) mode at low ultrasonic frequencies is used, when dealing with its propagation across the deposit, the product of the operating frequency f to the thickness h is a characteristic product that affects the physics. Several studies have been interested about the scattering and reflection from a many types of defects using guided waves in pipes [7–13].

The organization of this paper is described as follows: The theory about generation and propagation of guided waves in cylindrical structures with the use of semi-analytical methods to plot dispersion curves is first presented. A numerical method based on this theory is then demonstrated by applying the suitable type of excitation of the T(0,1) mode. Lastly, we propose a SHM approach to quantify the thickness evolution of the resin deposit and a NDT method to locate the deposit and dimension its extent.

2 Ultrasonic waves in cylindrical guide

2.1 Theory

Cylindrical structures like pipes, thin rods, capillaries, tubes, etc. support the propagation of mechanical waves at ultrasonic frequencies along their axes. The waveguide behaviour is used in several engineering applications and widely in the NDT domain of the SHM of tubular structures. The calculation of the acoustic modes in an isotropic cylinder is best done with the potential method [14].

The wave equation and potential functions are expressed in cylindrical coordinates (r, θ, z) and the solutions for the potentials and displacements are found in terms of Bessel functions. Displacement components are u_r and u_θ in the section of the cylinder and u_z along its length. The boundary conditions for the three components of stress at the free surface σ_{rr}, $\sigma_{r\theta}$, and σ_{rz} must set equal to zero. The determinant of the coefficients is set equal to zero and the dispersion equation can be solved numerically. The result is that there are three families of modes, which can be described as follows:

Compressional or longitudinal modes L(0,n), which are axially symmetric with displacements u_r and u_z independent of θ. The dispersion relation (PC equations), qualitatively resembles Lamb waves where the fundamental mode goes to a constant velocity (bar velocity c_b) expressed as $c_b = \sqrt{E/\rho}$. E represents the Young's modulus and ρ is the density. The other modes all have cut-off frequencies and are dispersive.

Torsional modes T(0,n) : There is only one displacement component, u_θ, which is independent of θ. In addition, the fundamental mode is not dispersive and propagates with a constant velocity (shear bulk velocity c_s) $c_S = \sqrt{\mu/\rho}$ where μ is the shear modulus. The higher-order modes are dispersive and have all cut-off frequencies. The dispersion curves for the whole family of torsional modes resemble those for SH modes in a plate.

Flexural modes F(m,n) : These modes are the most complicated as they involve displacement components u_r, u_θ, and u_z, which vary with θ as $\sin(n\theta)$ and $\cos(n\theta)$. These modes qualitatively resemble the antisymmetric modes of a plate. In particular, the fundamental has no cut-off and propagates down to zero frequency, while the higher modes have cut-offs and are dispersive.

2.2 Dispersion curves

The two fundamental characteristics of a waveguide are the discretization of waves into propagating modes and the existence of dispersion. Only a finite number of propagating modes are permitted for a given frequency, and whose properties are determined by the configuration of the cross section and boundary conditions of the waveguide. The dispersion consists on the nonlinear relationship between wavenumber and frequency. From there, signals with a significant bandwidth are distorted as they propagate along the waveguide because of their spectral components which propagate at different phase velocities.

The dispersion curves are obtained by solving the PC frequency equations by using SAFE techniques. The SAFE formulations approach reduces the three dimensional wave propagation problem to a one or two dimensional for a cylindrical guide for example with a considerable reduction of computational time and

memories needs. From a numerical point of view, the SAFE techniques have some advantages compared to software tools based on a theoretical description of the wave propagation like DISPERSE [15] which is the most reliable. Nevertheless, SAFE techniques cannot predict the dispersive behaviour of leaky guided waves, whereas the analytically based software can.

Two powerful software based on the SAFE techniques, GUIGUW [16–17] and PCDISP [18], may be used to plot quickly the dispersion curves of a cylindrical single or multilayered waveguide made of several type of materials. We use PCDISP which is a Matlab® open source toolbox approximating solutions derived from numerical methods of the PC equations with a length of the guide infinite along its *z*-axe. In Figure 1 the dispersion curves for an aluminum hollow cylinder with an inner radius r_{in} = 10mm and outer radius r_{out} = 12mm are plotted.

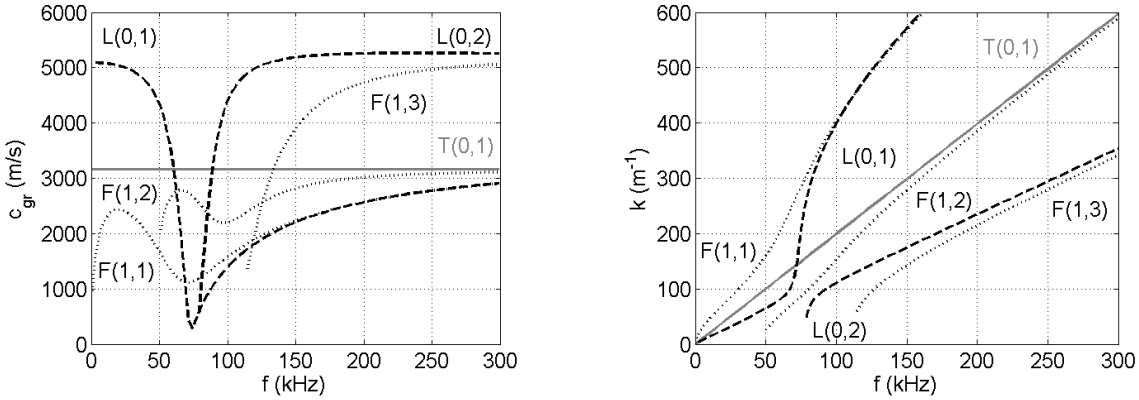

(a) (b)

Figure 1: Dispersion curves for an aluminum tube of 10mm inner radius and 12mm outer radius. Group velocity (a) and wavenumber (b) versus frequency

The three families of guided waves can propagate in the frequency range of 0 – 300kHz. For longitudinal modes (black dashed lines), two exist. The fundamental mode L(0,1) presents a non-dispersive region with a group velocity c_{gr} =5090 m/s equal to the bar velocity in very low frequencies. The consecutive higher order mode L(0,2) with a cut-off frequency at approximately f = 80kHz presents also a non-dispersive region from f = 150kHz. The first three flexural modes F(1,1), F(1,2), and F(1,3) (black dotted lines) exist in the frequency range, they are all dispersive. Only the fundamental mode F(1,1) has no cut-off frequency. For the torsional modes (gray solid line), only the fundamental one T(0,1) with a group velocity (c_{gr} =3150 m/s) equal to the bulk shear wave velocity of aluminum, can propagate in the frequency range. It presents no cut-off frequency and is also non-dispersive.

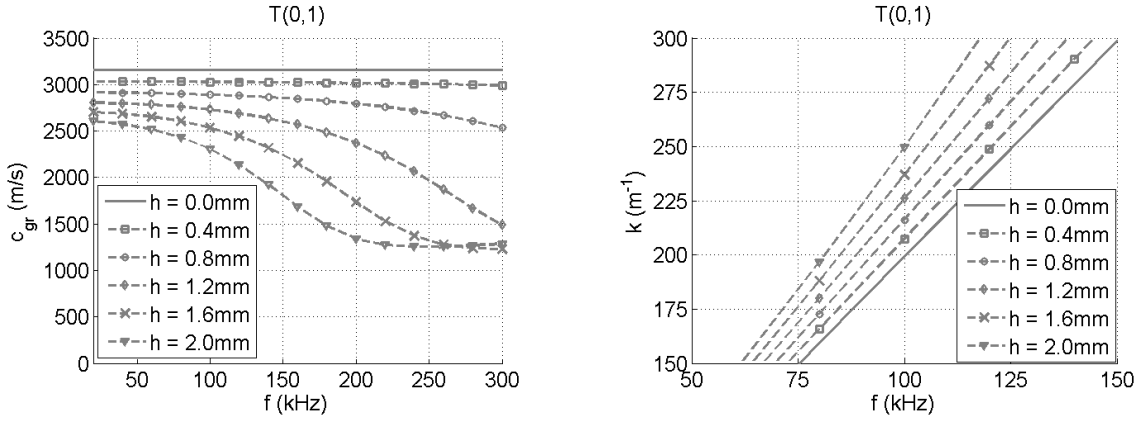

(a) (b)

Figure 2: T(0,1) mode dispersion curves for an aluminum tube (solid line) and bilayers aluminum-resin of thicknesses *h* (dashed lines). Group velocity (a) and wavenumber (b) versus frequency.

3 Finite Element Method (FEM) simulations

The FEM analysis is a widely used numerical solution approach for solving problems of wave propagation and vibration. For solving the PC equations without analytical solutions, FEM can provide accurate and computationally efficient solutions that may be improved by refining the elements used in the study. FEM may be combined with analytical analysis or other numerical methods to achieve optimum solutions. Usually a successful FEM simulation involves the following items:
Problem classification: physics to be analysed
Mathematical modeling: including geometries, governing equation, appropriate solving approaches
Discretization: dividing a mathematical model into a mesh of finite elements
Preliminary analysis: having some analytical results, experience, or experimental results for comparison
Finite element analysis:

Pre-processing: inputting data of geometry, material properties, boundary conditions, etc.

Numerical calculation: deciding interpolation functions, obtaining a matrix to describe the behaviour of each element, assembling these matrices into a global matrix equation, and solving this equation to determine the results

Post-processing: listing or graphically displaying the solutions

Check the results: making sure that the FEM simulation has been carried out correctly and then comparing the FEM results to the preliminary analysis.

In this paper, the commercial FEM software Comsol Multiphysics© is used to conduct the ultrasonic wave propagation in cylindrical waveguides. The *Structural Mechanics* module and its *Temporal Analysis* item are chosen to build the 3D model to simulate the wave propagation at the operating frequency f = 100 kHz. To achieve the accuracy of the FEM simulation, we check the calculation results based on both theoretical research (dispersion curves with PCDISP). The properties of the materials used in the following simulations and their dimensions are summarized in Table 1 below where h represents the thickness the resin layer which grows from 0mm to 2mm by a step of 0.4mm.

Material	Inner radius r_{in} (mm)	Outer radius r_{out} (mm)	Length (mm)	Density ρ (kg.m^{-3})	Young's modulus E (GPa)	Poisson's ratio ν
Aluminum	10	12	900	2700	70	0.33
Resin	12	12 + h	100	1090	5.5	0.18

Table 1: Material properties and geometry of the different layers

3.1 Wave generation and propagation

Torsional modes are characterized by a polarization around u_θ and they propagate along the u_z axe. In order to simulate the propagation of the fundamental torsional mode T(0,1) at the operating frequency (f = 100kHz) in a SHM-type approach, we need to define a time dependent source excitation along the waveguide. As illustrated in Figure 4, the sources are located at the position z = 0mm around the outer circumference with an axially symmetric distribution. An array of four points **PT#*n*** with n = 1, 2, 3 and 4 excited by a time-dependent load generating the tangential and ortho-radial movement. The excitation for all the four points is a five-cycle Hanning windowed tone burst signal as defined in Eq (1) by:

$$s(t) = A\left[1-\cos\left(\frac{2\pi ft}{n}\right)\right]\cos(2\pi ft).\left(t \le \frac{n}{f}\right) \quad (1)$$

where the amplitude is set to A = 1, the number of signal cycles n = 5 and also the center frequency f = 100kHz as defined above. Modulating a signal by a Hanning window is commonly used in the domain of ultrasonic NDT/E, it allows us to reduce energy dispersion away from the central excitation frequency.

The time amplification factor $s(t)$, with a duration of 50µs is plotted in Figure 3(a) and the normalized magnitude of its Fast Fourier Transform (FFT) $|S(f)|$ plotted in Figure 3(b) shows that the signal energy is centered at the frequency excitation of 100kHz.

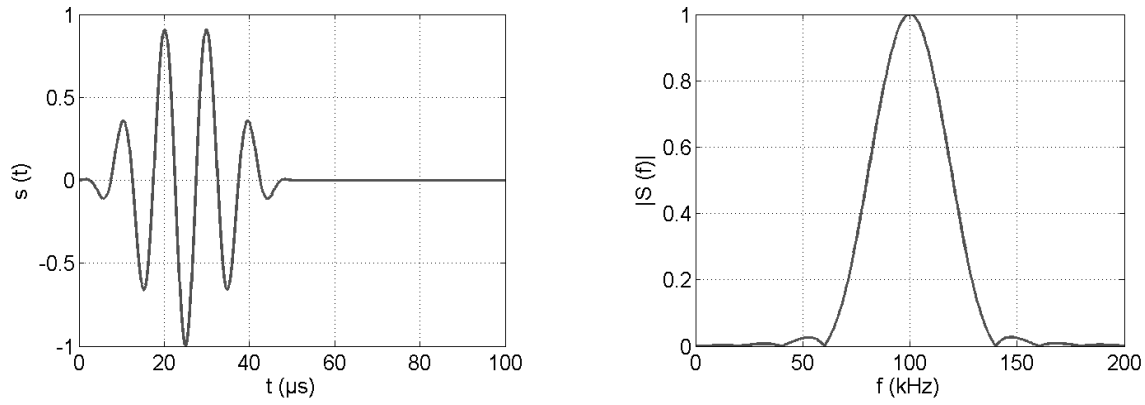

(a) (b)

Figure 3: Excitation signal with a 5-cycle Hanning-windowed tone burst centered at f = 100kHz. Temporal signal (a) and normalized spectrum (b).

As illustrated in the dispersion curves, the T(0,1) mode for a single layer of aluminum presents any dispersion with the frequency. On the other hand, for bilayers aluminum-resin, the T(0,1) mode at f = 100kHz becomes dispersive when h increases. This dispersion is more significant towards the higher frequencies (f > 150kHz). By choosing the excitation frequency of f = 100kHz, we make sure to generate only the T(0,1) mode allowing us to an easier interpretation of the resulting time-transient responses.

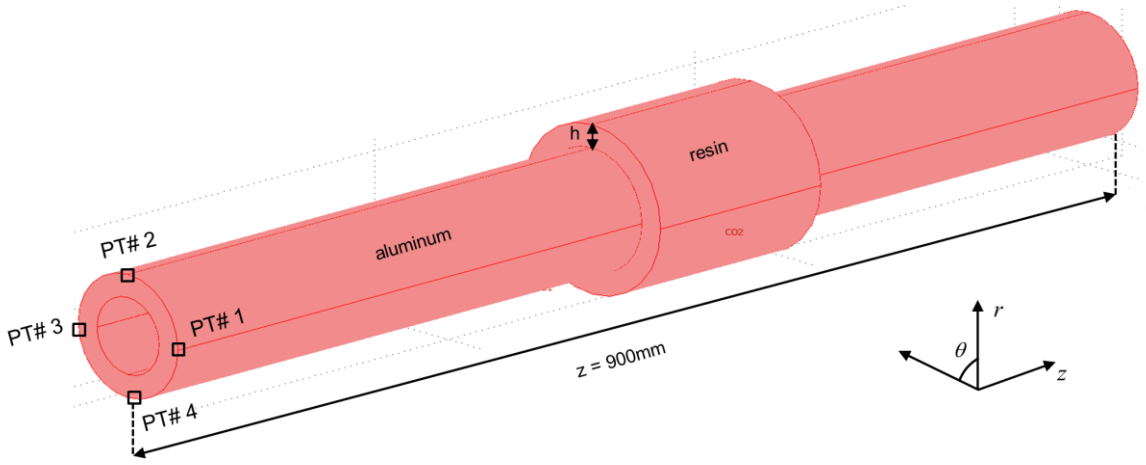

(a)

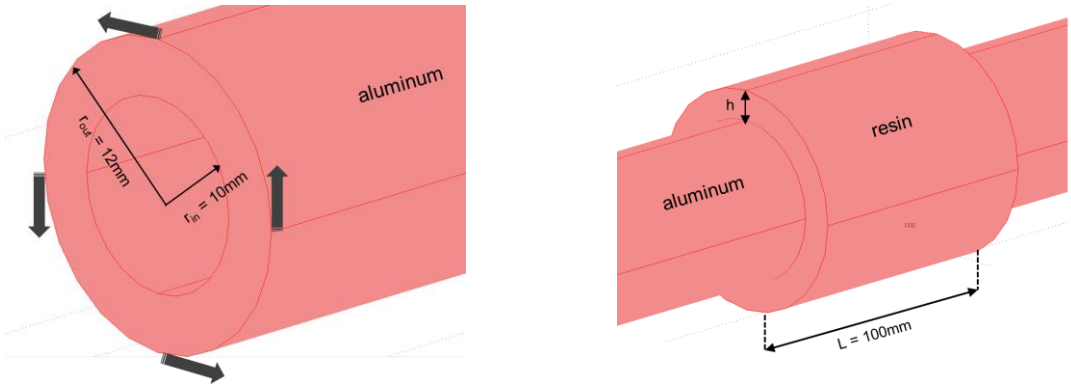

(b) (c)

Figure 4: Full length schematic of the 3D model (a). Excitation applied in circumferential direction at each point PT(b), zone of the aluminum tube surrounded by resin layer(c).

Six simulations are conducted, one for a single aluminum tube (h = 0mm) and five other for the defective ones with a resin layer of length L = 100m, a thickness growing from h =0.4, 0.8, 1.2, 1.6 and 2mm (Figure 4(c)).

As introduced before, the *Structural Mechanics* module with the *Time Transient Analysis* is used to model the propagation of the fundamental T(0,1) mode along the tubes. For accurate analysis of wave propagation in a fully 3–D model, a suitable mesh size is required. Several studies often used approximate theories such as the shell theory or assumed axisymmetry to save computational cost [11–12]. The meshes used in the models were auto-setted by the software itself by 8 nodded cubic brick elements. In the case of the defective samples, the mesh is more refined in the defective area. In both cases the mesh is sufficiently fine to provide a converged solution for the propagation of the T(0,1) mode.

With a distance of propagation z = 900mm, the duration of a round-trip echo of the T(0,1) mode along the waveguide is approximately 600µs. Then we fix the duration of the simulations at the time t = 700µs with an iteration step of $\Delta t = 1e^{-7}$s, based on the stability criterion for an explicit time marching scheme in term of the fastest velocity in the frequency range.

In Comsol Multiphysics© the displacement wavefield along the r, θ and z direction can be extracted at any time. For visualizing the T(0,1) mode, the ortho-radial displacements u_θ along the z-axis are collected and represented in the form of B-scan images.

3.2 B-scan imaging

The displacement amplitudes u_θ varying as a function of time are stored for each position z at the external surface in term of a matrix $s(z, t)$. For example, the simulation results for the aluminum tube (Figure 5(a)) and bilayer with h = 0.8mm (Figure 5(b)) are presented in the form of B-scan images, defining the amplitude distribution of the u_θ displacements. The displacement amplitudes are given in gray level versus time t and position z and it can be observed that only the T(0,1) mode is propagating along the different waveguides.

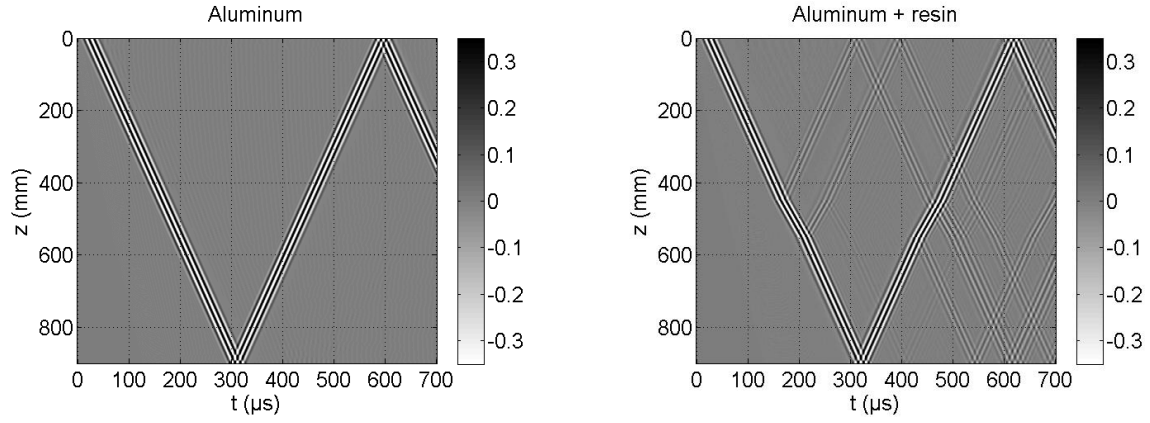

(a) (b)

Figure 5: B-scan images of the T(0,1) mode propagation for the aluminum tube (a) and aluminum tube surrounded by a resin deposit with h = 0.8mm(b).

In both simulation cases, it should be noted that the B-scan images have been acquired in a relatively long time interval, with duration of 700µs. One can see also that the time required for the generated T(0,1) mode to be reflected by the opposite edge (z = 900mm) is evaluated at about t = 300µs. Therefore, the round trip echo of the mode is doubled (i.e. t = 600µs). By observing the B-scan image of the Figure 5(b) one can see that multiple reflections are clearly visible. These reflected echoes arise from the interaction of the generated mode propagating in the structure with a discontinuity. Two reflections are noted respectively at z = 450mm and 550mm corresponding to the boundaries of the defect with length L = 100mm in the structure.

On the basis of the simulation results, it has been found that the group velocity of the T(0,1) mode in the aluminum tube is constant (c_{gr} = 3150m/s). By looking closely at the B-scan image of the defect, a slope variation of the wave fronts can be observed between the instants t_1 = 167.8µs and t_2 = 202.4µs. This change in slope illustrates a variation of group velocity that is substantially equal to 2890 m/s in this region (i.e. due to the change in thickness).

4 SHM and NDT methods for detecting defect

After conducting these simulations, we propose a SHM method to quantify the evolution of the thickness h of the resin layer (defect) and a NDT method to determine its extent L.

4.1 Reflected wave energy evaluation

In order to carry out a study in the field of guided-wave-based SHM, we use a method based on measuring the time of arrival, currently utilized in experimental configuration. It consists of using a transducer ring working as an actuator and sensor of guided waves. So numerically the same method of analyze can be realized with the obtained B-scans. By making cuts at any position z along the structures, it is possible to plot the temporal signals (A-scans). We decided to carry out a transmission/reception (T/R) analysis that consists of plotting a cut at the position z = 0mm in the different B-scan images. Figure 6 shows the time-transient responses at this position (displacement amplitudes u_0) for the aluminum tube (h = 0mm) and bilayers with h = 0.8 and 2mm.

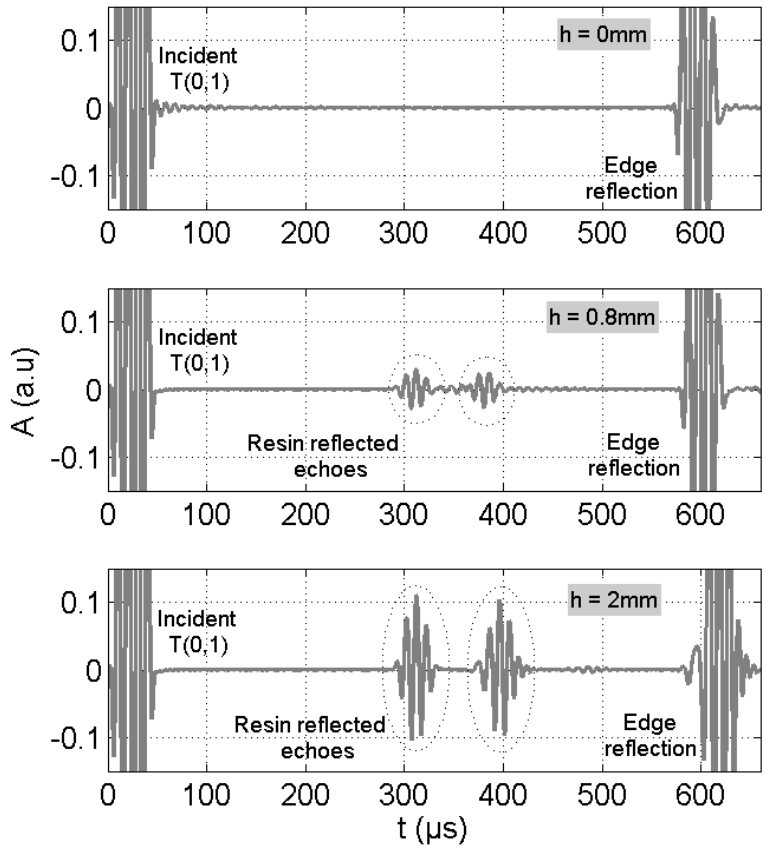

Figure 6: Time transient responses obtained at z = 0mm) for the simulated aluminum (h = 0mm) and aluminum + resin (h = 0.8mm and 2mm) structures.

It can be seen that only the T(0,1) mode is propagating along all the structures and any edge reflection pulse signal is lost. Another remark about these echoes is that they are not distorted. This observation illustrates the relatively or non-dispersive behaviour of this mode for long traveled distance (900mm). The first information to be carried out about the propagation of the T(0,1) mode in the aluminum tube (h = 0mm) is the determination of the time of flight required for the signal to travel from the excitation source to the right end of the tube and back again is t_f = 595.4µs. This time of flight t_f is evaluated at 601.4µs and 619.2µs for the two other plotted time-transient signals respectively with h = 0.8mm and 2mm. As for now, we can note that signal arrivals are slightly affected and increase when h becomes greater. The second information found is the appearance of two wave packets between the incident and the edge reflected waves when h become non-zero. These echoes come from the reflections due to the resin layer. The arrival time of the first

packet occurs at t_3 = 311.2µs whatever the value of h (Figure 7(a)) and they are obtained by plotting the Hilbert envelopes of all the A-scans. With this time arrival the distance d from the source (z = 0mm) to the left end position of the resin layer is evaluated by $d = c_{gr} \times (t_3 – t_0)/2$ = 450mm where the group velocity of aluminum c_{gr} = 3150m/s and t_0 = 25µs corresponding to the maximum of the Hilbert envelop of the incident T(0,1) mode signal. The second wave packet which corresponds to the right end resin layer reflection appears at different time t_4 depending on h (group velocity). More h is increasing (i.e. less c_{gr} is decreasing), more this echo appears later over the time.

Therefore, in an SHM-type approach, any echo appearing in the analysis window between the emission echo and the echo reflected from the end of the tube is caused by the reflection of an anomaly in the tube. With the simulations carried out here, in order to quantify the evolution of the thickness h of the resin layer, we evaluate the energies of the spectra of the different reflected signals. Theoretically the energy E of a signal $s(t)$ with its FFT $S(f)$ is expressed in the form of the integral described below:

$$E = \int_{t_b}^{t_e} \left| s(t) \right|^2 dt \qquad (2)$$

With these conditions, the defined time analysis window is between t_b = 50µs (end of the excitation time, i.e. t_0) and t_e = 590µs (beginning of the edge reflection echo of the tube). Figure 7(b) below, shows the evolution of this normalized energy E as a function of the thickness h.

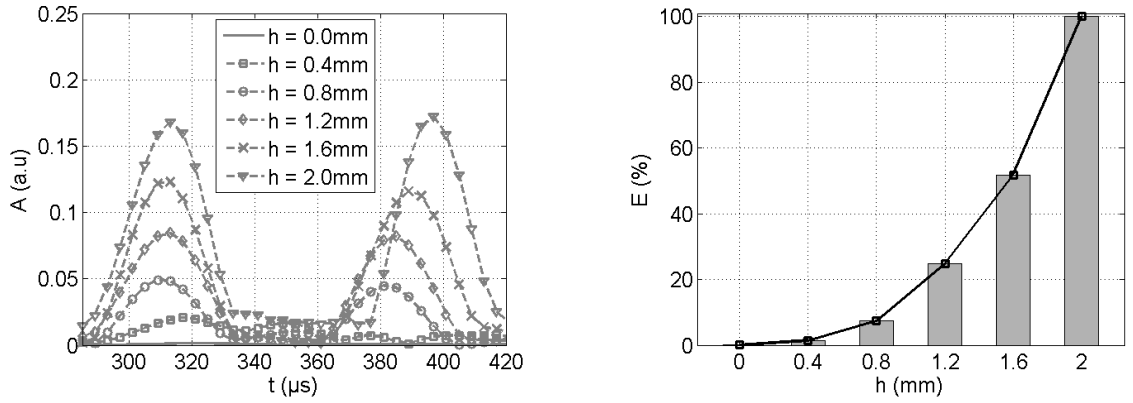

(a) (b)

Figure 7: Hilbert envelop of the reflected wave packets (a) and evolution of the normalized energy signal collected at the point source z = 0mm.

In Figure 7(a), it can already be seen that the amplitude of the echoes reflected by the resin increases considerably with the thickness h. The study realized on the energy shows that its normalized quantity increases quasi-monotonically when h also increases.

4.2 Defect length and thickness evaluation

The analysis of the various signals allowed us to see that the anomaly (presence of the resin layer) is distinguished by a change of the signal compared to the one obtained on the aluminum tube (reference signal). Herein, we propose a signal processing method based on the spatial Fast Fourier sliding window for locating and dimensioning this resin layer considered as a defect. This type of signal processing consists in isolating the wave fronts of the T(0,1) mode by filtering the different B-scan images and performing a first temporal FFT. The frequency is fixed at f = 100 kHz (the operating frequency) and then a window width to translate is defined. After these settings, we start to apply the spatial FFT at each position z with a Hanning window by a translation step of dz = 1mm. At the end of the processing, a position-wavenumber representation (z, k) is obtained. The results obtained on the aluminum tube alone (h = 0mm) and on the other structures aluminum + resin are illustrated in Figure 8.

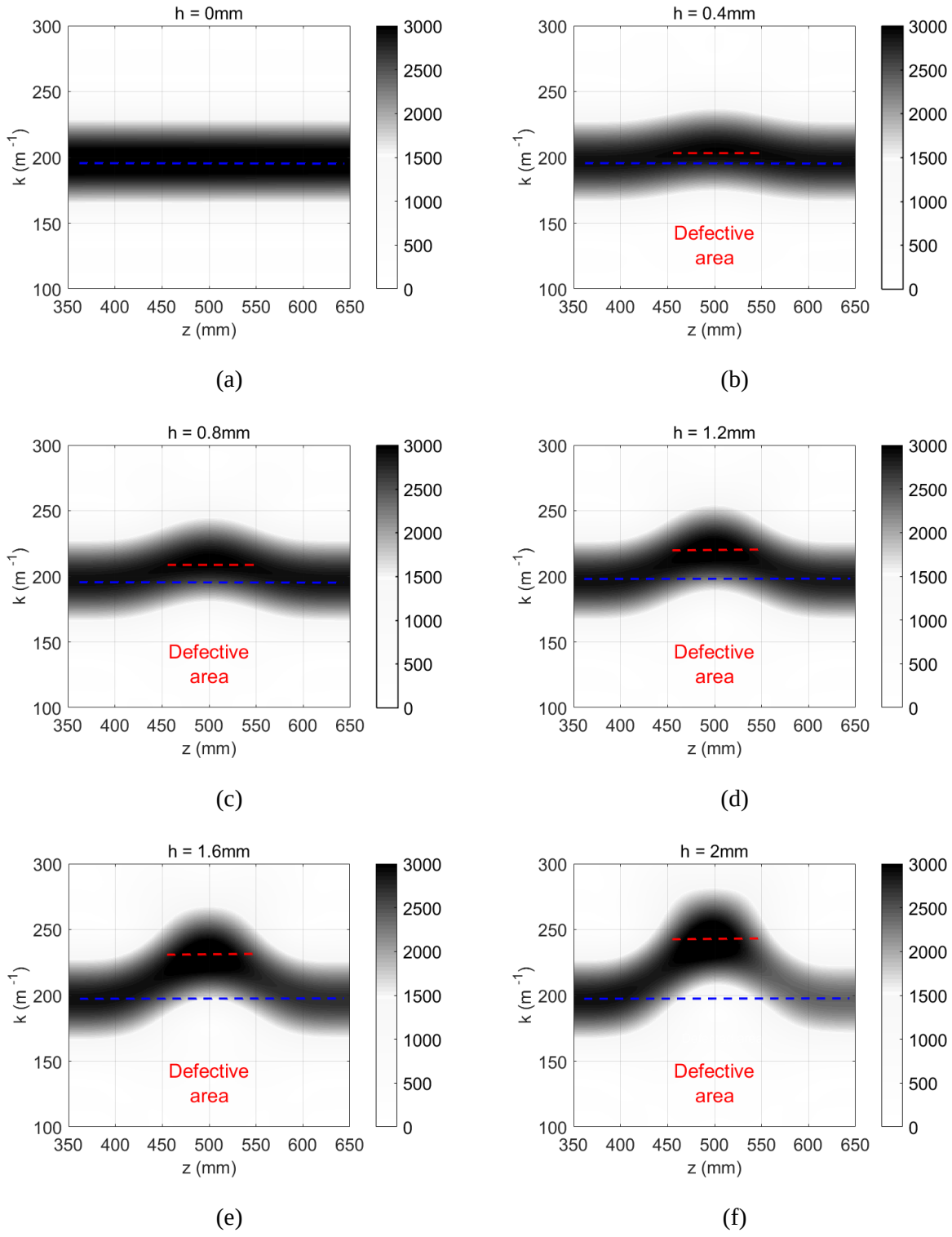

Figure 8: Spatial FFT with sliding window for detection and evaluation of corresponding wavenumber *k*.

These results allow us to determine the position *d* and the extent *L* of the resin layer (defect). Indeed, the extent *L* results in a variation of the wavenumber as a function of the distance *z*. If there is no resin (*h* = 0mm), the wavenumber remains constant with the value of $k = 198\text{m}^{-1}$ (blue dashed line) that represents the maximum of amplitude of the image (*z*, *k*). Now when *h* is non-zero, one can see that a discontinuity approximately between *z* = 450mm and 550mm (extent of the defect *L*) can be detected. The maximum of amplitude inside the elongated area corresponds to the wavenumber *k* (red dashed lines) of the corresponding bilayer aluminum + resin. When *h* increases, the wavenumber *k* increases (i.e. the group velocity c_{gr} decreases) and Table 2 below summarizes the values of *k* obtained by FEM method with Comsol Multiphysics© and those obtained by SAFE method with PCDISP.

Resin layer h (mm)	0	0.4	0.8	1.2	1.6	2
PCDISP k (m^{-1})	199	207.3	216.1	225.8	236.8	249.7
Comsol k (m^{-1})	198	206.7	213.3	221.8	231.9	243.9

Table 2: Comparison of the obtained wavenumbers by SAFE and FEM methods

These values of wavenumber obtained by spatial FFT with sliding windows prove the reliability of the signal processing because they can be compared with those obtained on the dispersion curves of the T(0,1) mode plotted in Figure 2(b) and reported in Table 2. Nevertheless, it can be observed that when the thickness h increases, dispersion is observed between the values obtained by SAFE method and those obtained by FEM method. This is due to the fact that with the SAFE method the length of the tubes is considered infinite along the z-axis whereas this is not the case in the FEM simulations (z = 900mm).

5 Conclusion

This paper is a contribution to the usefulness of FEM method as an intensive research topic in the field of guided-wave-based SHM. An array of four point sources is defined in order to generate the fundamental torsional T(0,1) guided wave over the entire circumference of aluminum tube surrounded or not by a resin layer.

First, we plot the analytical dispersion curves using the PCDISP free software and a large dispersion is noted when the thickness h of the resin layer increases. With Comsol, we simulate the propagation of the mode T(0.1) which is axisymmetric in a low dispersion region (f = 100kHz). The results of the simulations are represented in term of spatio-temporal images (B-scans) and one can observe that for the single aluminum tube alone, the wave fronts are not deviated during propagation. On the other hand, when h increases, the deviation of the wave fronts is more important. By currying out the temporal responses at the position z = 0mm (i.e. experimentally, in transmission/reception configuration), we obtain a round-trip echo which increases with h along the waveguide. When h is non zero, reflections are observed and quantified by evaluating their signal energies. The reflection also increases with h hence a quasi-monotonic energy evolution of the acquired signals as a function of the resin layer thickness is noted. A signal processing basing on the spatial FFT sliding window allowed us to dimension the extent of the resin layer as well as its thickness.

A comparison of the simulation results obtained with those obtained by the semi-analytical method shows a good agreement. These simulations carried out constitute an important tool on the guided wave control of tubular structures over time. Indeed various deposits may accumulate on their circumferences thus provoking their aging. From an experimental point of view, we can reproduce the simulation results obtained to monitor these structures by bonding piezoelectric patches (generation) and using laser scanning vibrometry (detection) with an application of the same signal processing to collected data.

6 References

[1] M. G. Silk and K. F. Bainton, ‘The propagation in metal tubing of ultrasonic wave modes equivalent to Lamb waves’, *Ultrasonics*, vol. 17, no. 1, pp. 11–19, Jan. 1979.

[2] J. L. Rose, J. J. Ditri, A. Pilarski, K. Rajana, and F. Carr, ‘A guided wave inspection technique for nuclear steam generator tubing’, *NDT E Int.*, vol. 27, no. 6, pp. 307–310, Dec. 1994.

[3] M. J. S. Lowe, D. N. Alleyne, and P. Cawley, ‘Defect detection in pipes using guided waves’, *Ultrasonics*, vol. 36, no. 1, pp. 147–154, Feb. 1998.

[4] D. C. Gazis, ‘Three-Dimensional Investigation of the Propagation of Waves in Hollow Circular Cylinders. I. Analytical Foundation’, *J. Acoust. Soc. Am.*, vol. 31, no. 5, pp. 568–573, May 1959.

[5] W. Luo and J. L. Rose, ‘Phased array focusing with guided waves in a viscoelastic coated hollow cylinder’, *J. Acoust. Soc. Am.*, vol. 121, no. 4, pp. 1945–1955, Apr. 2007.

[6] J. L. Rose, Y. Cho, and M. J. Avioli, ‘Next generation guided wave health monitoring for long range inspection of pipes’, *J. Loss Prev. Process Ind.*, vol. 22, no. 6, pp. 1010–1015, Nov. 2009.

[7] S. D. Akbarov and T. Kepceler, ‘On the torsional wave dispersion in a hollow sandwich circular cylinder made from viscoelastic materials’, *Appl. Math. Model.*, vol. 39, no. 13, pp. 3569–3587, Jul. 2015.

[8] S. D. Akbarov, T. Kepceler, and M. Mert Egilmez, ‘Torsional wave dispersion in a finitely pre-strained hollow sandwich circular cylinder’, *J. Sound Vib.*, vol. 330, no. 18–19, pp. 4519–4537, Aug. 2011.

[9] R. Carandente and P. Cawley, ‘The effect of complex defect profiles on the reflection of the fundamental torsional mode in pipes’, *NDT E Int.*, vol. 46, pp. 41–47, Mar. 2012.

[10] M. Castaings and C. Bacon, ‘Finite element modeling of torsional wave modes along pipes with absorbing materials’, *J. Acoust. Soc. Am.*, vol. 119, no. 6, pp. 3741–3751, Jun. 2006.

[11] A. Demma, P. Cawley, M. Lowe, and A. G. Roosenbrand, ‘The reflection of the fundamental torsional mode from cracks and notches in pipes’, *J. Acoust. Soc. Am.*, vol. 114, no. 2, pp. 611–625, Aug. 2003.

[12] A. Løvstad and P. Cawley, ‘The reflection of the fundamental torsional guided wave from multiple circular holes in pipes’, *NDT E Int.*, vol. 44, no. 7, pp. 553–562, Nov. 2011.

[13] W. Zhou, F.-G. Yuan, and T. Shi, ‘Guided torsional wave generation of a linear in-plane shear piezoelectric array in metallic pipes’, *Ultrasonics*, vol. 65, pp. 69–77, Feb. 2016.

[14] A. H. Meitzler, ‘Mode Coupling Occurring in the Propagation of Elastic Pulses in Wires’, *J. Acoust. Soc. Am.*, vol. 33, no. 4, pp. 435–445, Apr. 1961.

[15] B. Pavlakovic, M. Lowe, D. Alleyne, and P. Cawley, ‘Disperse: A General Purpose Program for Creating Dispersion Curves’, pp. 185–192, 1997.

[16] A. Marzani, ‘Time–transient response for ultrasonic guided waves propagating in damped cylinders’, *Int. J. Solids Struct.*, vol. 45, no. 25–26, pp. 6347–6368, Dec. 2008.

[17] P. Bocchini, A. Marzani, and E. Viola, ‘Graphical User Interface for Guided Acoustic Waves’, *J. Comput. Civ. Eng.*, vol. 25, no. 3, pp. 202–210, May 2011.

[18] F. Seco and A. R. Jimenez, ‘Modal analysis of the piezoelectric generation of ultrasonic guided waves for nondestructive testing of cylindrical structures’, *Russ. J. Nondestruct. Test.*, vol. 43, no. 10, pp. 683–691, Oct. 2007.